



AUSMPW+ 수치기법과 반응기체 모델을 이용한 극초음속 충격파-충격파 상호작용 수치해석

Numerical Analysis of Hypersonic Shock-Shock Interaction using AUSMPW+ Scheme and Gas Reaction Models

○ 이준호 ¹⁾, 김종암 ²⁾, 노오현 ²⁾

Joon-Ho Lee, Chongam Kim, and Oh-Hyun Rho

A two-dimensional Navier-Stokes code based on AUSMPW+ scheme has been developed to simulate the hypersonic flowfield of hypersonic shock-shock interaction. AUSMPW+ scheme is a new hybrid flux splitting scheme, which is improved by introducing pressure-based weight functions to eliminate the typical drawbacks of AUSM-type schemes, such as non-monotone pressure solutions. To study the real gas effects, three different gas models are taken into account in this paper: perfect gas, equilibrium flow and nonequilibrium flow. It has been investigated how each gas model influences on the peak surface loading, such as wall pressure and wall heat transfer, and unsteady flowfield structure in the region of shock-shock interaction. With the results, the value of peak pressure is not sensitive to the real gas effects nor to the wall catalyticity. However, the value of peak heat transfer rates is affected by the real gas effects and the wall catalyticity. The structure of the flowfield also changes drastically in the presence of real gas effects.

1. Introduction

1.1 Shock-Shock Interaction Problem

The heat transfer rates generated in the shock-shock interaction region can result in the large heating loads imposed on the thermal protection systems of hypersonic flight vehicles. In these regions, the sharply peaked heating rates are accompanied by high pressures.[1] The features of these interactions depend principally on the location of intersection between the impinging shock and bow shock around the blunt body like engine cowls. Edney[2] classified these interactions into six different patterns: Type I through Type VI.

The highest surface loading occurs in Type IV interaction, which is shown schematically in Fig. 1. This pattern is observed when the impinging oblique shock intersects the nearly normal portion of the cowl bow shock. This interaction creates a transmitted shock, which impinges on the lower bow shock. The flow crossing the upper bow shock is the freestream, while the flow crossing the lower bow shock and the transmitted shock has crossed the impinging shock. Behind the transmitted shock, a supersonic jet is formed and bounded by the shear layer, which passes through a series of weak oblique shocks and expansion fans. Finally, this jet impinges on the body surface, ending in a terminating strong shock. At this jet impinging point, very high surface heating and pressure peak exist. Behind the terminating shock, the subsonic flow is turned along the surface and then it becomes supersonic again when it is expanded over the body.

¹⁾ 한국항공우주연구원

²⁾ 서울대학교 항공우주공학과

(305-600, 대전시 유성우체국 사서함 113 호., Tel: 042-860-2000)
(151-742, 서울 관악구 신림동 산 56-1, Tel: 02-880-7380)

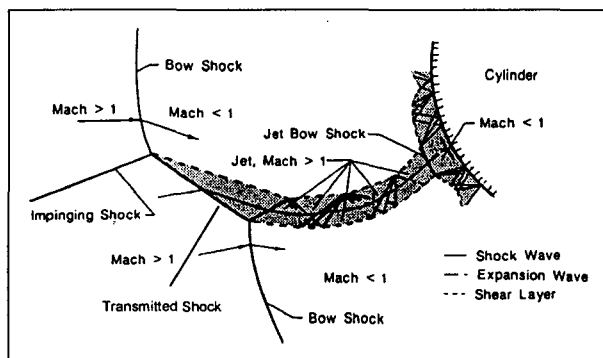


Fig. 1 Type IV interaction pattern[1]

1.2 Real Gas Effects on Shock-Shock Interaction Problem

Recently, three experimental studies have been conducted to investigate the influence of real gas effects on the aerothermal loads in regions of shock-shock interaction. In the experimental studies in the HEG piston driven shock tunnel by Kortz et al.[3], it is concluded that the structure of reacting gas is significantly different from the character of the perfect gas flow. These studies suggested that the peak heating and pressure levels are lowered by real gas effects as a result of an increase in scale of the interaction region. Similar conclusions were reached by Sanderson and Sturtevant[4] as a result of experiments in T5 piston driven shock tunnel.

In more recent experimental studies by Holden[5], measurements were made in LENS hypervelocity shock tunnel. The model was densely instrumented with high-frequency thin-film instrumentation to get a level of spatial and temporal resolution which exceeded those of the earlier studies. The measurements showed that the heat transfer rates were larger in the reacting flow, while reacting gas had a minor influence on pressure.

Several numerical analyses of reacting gas on the shock-shock interaction problem have been conducted using Navier-Stokes code. Steady type IV interaction problems were numerically studied by Prabhu *et al.*[6] for equilibrium chemistry. Zhong *et al.*[7] simulated unsteady type IV shock-shock interaction problems using five-species nonequilibrium model and a second-order TVD scheme together with a third-order semi-implicit Runge-Kutta method. They examined the real gas effects on the level of peak heating rates and pressures. Above numerical results suggest that real gas effects should enhance the peak heating rates.

1.3 Directions of the Present Study

The object of this study is to investigate the real gas effects on the surface loading, such as wall pressure and wall heat transfer, and on the structure of flowfield in hypersonic shock-shock interaction problem. To study the real gas effects, three different gas models are taken into account in this paper: perfect gas, equilibrium flow and nonequilibrium flow. It has been investigated how each gas model influences on the peak surface loading and unsteady structure of flowfield in the region of shock-shock interaction. Also, two kinds of boundary condition for wall catalyticity are taken into account in nonequilibrium calculation so that effects of wall catalyticity on the peak surface loading can be examined.

2. Governing Equations and Gas Models

2.1 Perfect Gas



A flow which is both chemically and vibrationally frozen has constant specific heats. This is nothing more than the flow of a calorically perfect gas.

2.2 Equilibrium Flow

When the density is sufficiently high so that there are sufficient collisions between particles to allow the equilibration of energy transfer between the various modes, the flow is in equilibrium. For an equilibrium flow, any two thermodynamic properties can be used to define the state of flow uniquely. In the present study, the thermodynamic properties such as pressure, enthalpy and temperature in equilibrium state, are calculated using the curve fitted data by Srinivasan, Tannehill and Weilmuenster [8]. The transport properties such as viscosity and conductivity, are calculated using the curve fitted data by Gupta *et al.* [9].

2.3 Nonequilibrium Flow

In the present paper, five-species chemical reaction model is used for the nonequilibrium flow calculation in the temperature range of $2500K < T < 9000K$ [10]. This model does not include any ionization, so it leaves five neutral species, N_2 , O_2 , NO , N , and O , to be considered. Blottner's model[11] is selected for the reaction rate constant.

Detailed formulation of each gas model is described in Ref. 12.

3. Numerical Methods

A two-dimensional Navier-Stokes code based on AUSMPW+(AUSM by Pressure-based Weight function +) scheme has been developed to simulate the hypersonic flowfield of shock-shock interaction. AUSMPW+ scheme is an improved scheme which eliminates the non-monotone pressure solutions, which is a typical drawback of AUSM-type schemes. Furthermore, AUSMPW+ shows a good accuracy in the prediction of wall properties such as wall heating rate due to its less numerical dissipation. In the analysis of shock-shock interaction problem, it is very important to predict the unsteady fluctuation of wall pressure and heat transfer accurately, and thus AUSMPW+ is chosen as a spatial discretization scheme in the present study. AUSMPW+ algorithm is described in detail in Ref. 13,14.

4. Results

4.1 Validation Problem

This is a typical validation problem for the analysis of shock-shock interaction; it has been solved numerically by many researchers because the experimental data of wall heat transfer and pressure are provided by Holden *et al.*[1].

Figure 2 and figure 3 are computed results of instantaneous wall pressure and heat transfer compared with experimental data by Holden *et al.*[1]. The abscissa θ is the angle measured with respect to the horizontal, the negative values denoting the cylinder surface below the non-interacting stagnation streamline. The value of pressure is normalized by the undisturbed stagnation pressure obtained from the Rayleigh supersonic pitot pressure formula, which is 8.141×10^4 N/m². The undisturbed stagnation heat transfer value predicted theoretically by Fay and Riddell is 4.42×10^5 W/m², which is used to normalize the values of wall heat transfer. Computed results are in good agreement with experimental data.

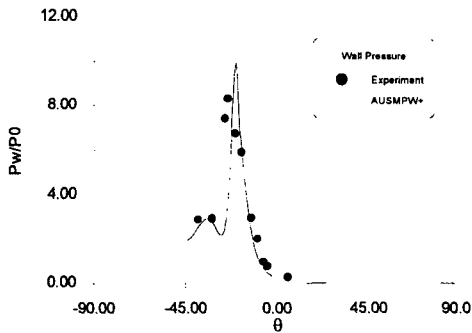


Fig. 2 Wall pressure distribution

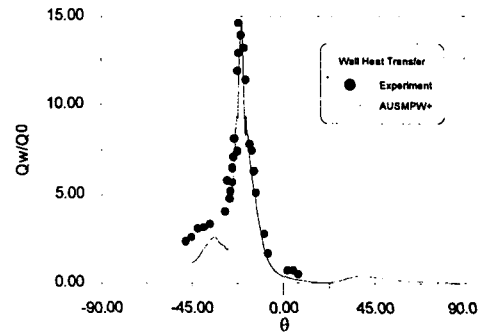


Fig. 3 Wall heat transfer distribution

4.2 Real Gas Effects on Shock-Shock Interaction Problem

One of the experimental conditions in Ref. 5 is taken: Run 61 for the air at the total enthalpy level of 10 MJ/kg. Freestream values of Run 61 are given in table 1.

Table 1 Freestream values of Run 61 for air at the total enthalpy level of 10 MJ/kg[5]

Reynolds number [1/m]	4.938E5
Wall temperature [K]	296.91
Cylinder radius [m]	0.0381
Mach number	8.53
Velocity [m/sec ²]	4420.5
Temperature [T]	670.11
Pressure [N/m ²]	709.63
Density [kg/m ³]	3.6195E-3
Angle of attack [deg]	0.0

This case of shock-shock interaction problem is numerically analyzed with different gas models. Figure 4 and figure 5 show wall pressure and heat transfer distributions. It is obvious that the value of peak pressure does not affected by the choice of gas models. Almost the same values are predicted in all cases. However, there are noticeable differences between the peak values of heat transfer in Fig. 5. It is observed that the peak heating levels are increased by about 150-180 percent compared with perfect gas heating levels when equilibrium flow model or nonequilibrium flow model with the catalytic wall is used. Nonequilibrium flow model with the noncatalytic wall predicts slightly higher value of heat transfer peak than perfect gas model. It is concluded that the value of peak heat transfer rates is affected by the reacting gas models and the wall catalyticity.

In Fig. 4 and Fig. 5, it is observed that the location of peak surface loading in perfect gas flow moves downwards compared with those in reacting gas flows. This is related to the difference of shock stand-off distance accompanied by the gas model, which is clearly seen in the flow contours. Mach number contours with difference gas models are shown in Fig. 6. The shock stand-off distance becomes shorter when gas reactions occur. Therefore, the intersection point between the impinging shock and upper bow shock moves toward the cylinder and upwards. Subsequently, the impinging jet also moves towards the cylinder and upwards, so it impacts on the wall at the upper point than in the perfect gas flow. This is why the locations of peak pressure and



heat transfer move upwards on the surface in case of the reacting gas flow.

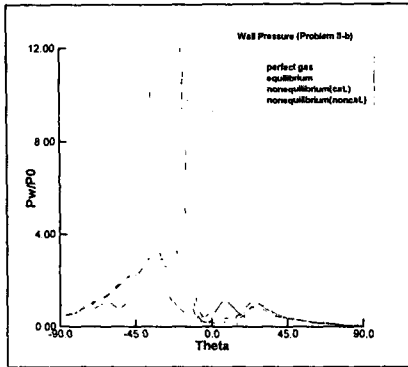


Fig. 4 Wall pressure distribution

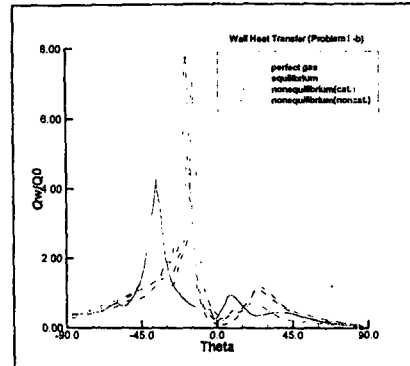


Fig. 5 Wall heat transfer distribution

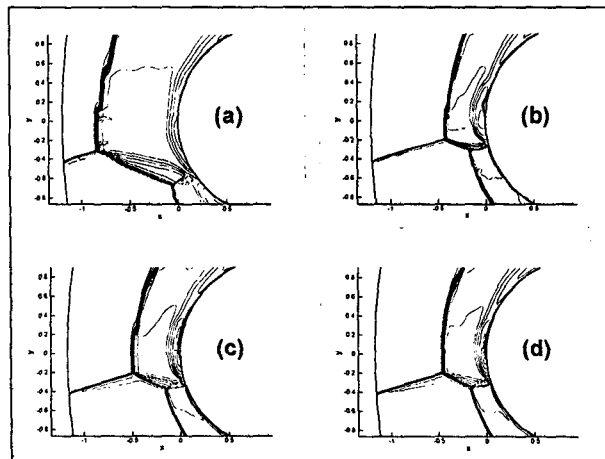


Fig. 6 Mach number contours with different gas models

(a) perfect gas, (b) equilibrium flow, (c) nonequilibrium flow, catalytic wall and (d) nonequilibrium flow, noncatalytic wall

5. Conclusions

Numerical analysis of hypersonic shock-shock interaction has shown the following results:

- (1) When AUSMPW+ scheme has been applied in the numerical analysis of shock-shock interaction problem, it can predict the peak values of surface pressure and heat transfer accurately, as well as the unsteady mechanism of shock-shock interaction.
- (2) The value of peak pressure is not sensitive to the real gas effects nor to the wall catalyticity. It is observed that almost the same values of peak pressure are obtained whether gas reactions are present or not.
- (3) The value of peak heat transfer rates is affected by the real gas effects and the wall catalyticity. It is observed that the peak heating levels are increased by about 150 to 180 percent compared with perfect gas heating levels when equilibrium flow model or nonequilibrium flow model with the catalytic wall is used. Nonequilibrium flow model with the noncatalytic wall predicts slightly higher value of heat transfer peak than perfect gas model.



- (4) The structure of the flowfield changes drastically in the presence of real gas effects. There is a dramatic decrease in shock stand-off distance in the reacting gas case compared with an perfect gas case. This change of shock stand-off distance moves the location of intersection point between the impinging shock and upper bow shock towards the cylinder and upwards, and subsequently moves the location of jet impinging point upwards on the surface. Therefore, the location of peak pressure and heat transfer on the surface is also moved to the upper points in case of reacting gas, compared with a perfect gas case.

References

- [1] Holden, M. S., Wieting, A. R., Moselle, J. R. and Galss, C., "Studies of Aerothermal Loads Generated in Regions of Shock/Shock Interaction in Hypersonic Flow," AIAA Paper 88-0477, 1988.
- [2] Edney, B. "Anomalous Heat Transfer and Pressure Distributions on Blunt Bodies at Hypersonic Speeds in the Presence of an Impinging Shock," Aeronautical Research Inst.of Sweden, FFA Rept. 115, Stockholm, Sweden, Feb. 1968.
- [3] Kortz, S., McIntyre, T. J. and Eitelberg, G., "Experimental Investigation of Shock-on-Shock Interactions in the High-Enthalpy Shock Tunnel Göttingen (HEG)," *Shock Waves at Marseilles I, Hypersonics, Shock Tube and Shock Tunnel Flow, Proceeding Marseilles, France*, 1993.
- [4] Sanderson, S. R. and Sturtevant, B., "Shock-Interference Heating in Hypervelocity Flow," *Proceedings of the 20th International Symposium on Shock Waves, Volume I*, World Scientific, Pasadena, CA, July 1995.
- [5] M. S. Holden, "Real Gas Effects on Regions of Viscous-Inviscid Interaction in Hypersonic Flows," AIAA Paper 97-2056, 1997.
- [6] Prabhu, R. K., Stewart, J. R. and Thareja, R. R., "Shock Interference Studies on a Circular Cylinder at Mach Number 16," AIAA Paper 90-0606, 1990.
- [7] Furumoto, G. H. and Zhong, X., "Numerical Simulation of Viscous Unsteady Type IV Shock-Shock Interaction with Thermochemical Nonequilibrium," AIAA Paper 97-0982, 1997.
- [8] Srinivasan, S., Tannehill, J. C. and Weilmuenster K. J., "Simplified Curve Fits for the Thermodynamic Properties of Equilibrium Air," NASA RP-1181, Aug. 1987.
- [9] Gupta, R. N., Lee, K. P., Thompson, R. A., and Yos, J. M., "Calculations and Curve Fits of Thermodynamic and Transport Properties for Equilibrium Air to 30000 K," NASA RP-1260, 1991.
- [10] Candler, G. V., "The Computation of Weakly Ionized Hypersonic Flows in Thermo-Chemical Nonequilibrium," Ph.D. Thesis, Stanford Univ., 1988.
- [11] Gupta, R. N., Yos, J. M., Thompson R. A. and Lee, K. P., "A Review of Reaction Rates and Thermodynamic and Transport Properties for an 11-Species Air Model for Chemical and Thermal Nonequilibrium Calculations to 30,000K," NASA RP-1232, 1990.
- [12] Lee, J. H., "Numerical Analysis of Hypersonic Shock-Shock Interaction Using AUSMPW+ Scheme and Gas Reaction Models," Ph. D. Thesis, Seoul National Univ., 1999.
- [13] Kim, K. H., Lee, J. H. and Rho, O. H., "An Improvement of AUSM Schemes by Introducing the Pressure-Based Weight Functions," *Computers and Fluids*, Vol. 27, No. 3, 1998, pp.311-345.
- [14] Kim, K. H., Kim, C. and Rho, O. H., "Accurate Computations of Hypersonic Flows Using AUSMPW+ Scheme and Shock-Aligned Grid Technique," AIAA Paper 98-2442, 1998.